

SEISMIC PERFORMANCE ASSESMENT OF A PERUVIAN PUBLIC SCHOOL “MODULE 780-ACTUAL” USING NONLINEAR STATIC AND DYNAMIC ANALYSIS

EVALUACIÓN DEL DESEMPEÑO SÍSMICO DE UN COLEGIO PÚBLICO PERUANO “MODULO 780-ACTUAL” USANDO ANÁLISIS NO LINEAL ESTÁTICO Y DINÁMICO

Gianfabio Pérez ^{1*}, Illarick Balarezo ^{2,3}, George Gonzales ³

¹ Facultad de Ingeniería Civil, Universidad Privada de Tacna, Tacna, Perú

² Laboratorio de Métodos Numéricos en Ingeniería (LMNI-LAME), Facultad de Ingeniería, Universidad de Buenos Aires, Buenos Aires, Argentina

³ Facultad de Ingeniería Civil, Universidad Peruana de Ciencias Aplicadas (UPC), Lima, Perú

Recibido (Received): 01 / 01 / 2025 Aceptado (Accepted): 01 / 01 / 2025

ABSTRACT

The seismic zone of Peru is at the convergence boundary between the Nazca and South American plates. This interaction, known as a subduction zone, is responsible for the major historical earthquakes recorded over the past four centuries, with magnitudes reaching up to 8.8 Mw. For this reason, it is crucial to evaluate the seismic performance of essential buildings, such as the Peruvian public school “Module 780-Actual,” which features a structural system combining reinforced concrete walls in the longitudinal direction and confined masonry in the transverse direction. This study proposes a methodology to assess the seismic performance of educational institution No.22459, built in 2010 and located in the Ica region. For this purpose, confined masonry walls were idealized using diagonal compression struts, calibrated with concentrated plastic hinges at their mid-length. Additionally, distributed plasticity fiber models were employed for columns, while concentrated plasticity models were used for beams. The nonlinear static analysis (pushover) was conducted to determine the capacity curve and identify the performance point. Pushover analysis results were compared with those obtained through a nonlinear dynamic analysis, which utilized representative seismic records from the national territory. Both approaches showed good agreement. In conclusion, the seismic performance of the structure in both evaluated directions achieved the “Life Safety” level for a maximum considered earthquake with a return period of 2475 years. The proposed methodology may be considered a viable approach for preliminary evaluations of seismic performance in regular, low-rise structures incorporating confined masonry, using the pushover analysis as the primary tool.

Keywords: Seismic Performance, Nonlinear Analysis, Confined Masonry

RESUMEN

La zona sísmica de Perú se sitúa en el límite de convergencia entre las placas de Nazca y Sudamericana. Este contacto, denominado zona de subducción, es responsable de los grandes terremotos históricos registrados en los últimos cuatro siglos, con magnitudes de hasta 8.8 Mw. Por esta razón, resulta de vital importancia evaluar el desempeño sísmico de las edificaciones esenciales, como el colegio público peruano “modulo 780-actual”, que cuenta con un sistema estructural que combina muros de concreto armado en la dirección longitudinal y albañilería confinada en la dirección transversal. Este trabajo propone una metodología para evaluar el desempeño sísmico de la institución educativa No.22459, que fue construida en el año 2010 y está ubicada en la región de Ica. Para lo cual, se idealizó los muros de albañilería confinada a través de puntales diagonales en compresión, previamente calibrados con rótulas concentradas ubicadas en su punto medio. Además, se utilizaron modelos de plasticidad distribuida tipo fibra para las columnas y plasticidad concentrada para las vigas. El análisis no lineal estático (pushover) permitió determinar la curva de capacidad y localizar el punto de desempeño. Los resultados del análisis pushover se compararon con los obtenidos mediante un análisis no lineal dinámico, en la cual se utilizaron registros sísmicos representativos del territorio nacional. Ambos enfoques mostraron una buena concordancia. En conclusión, el desempeño sísmico de la estructura, en ambas direcciones evaluadas, alcanza el nivel de “resguardo de vida” para un sismo máximo considerado de 2475 años. La metodología propuesta puede considerarse un enfoque viable para evaluaciones preliminares del desempeño sísmico en estructuras regulares y de baja altura que incorporen albañilería confinada, utilizando el análisis pushover como herramienta principal.

Palabras Clave: Desempeño Sísmico, Análisis No Lineal, Albañilería Confinada

¹ * Corresponding author:
E-mail: gianfabiopg@gmail.com

1. INTRODUCTION

Peru is a country with high seismic activity, particularly in the central coastal region, where the recurrence interval for a similar event to the 1746 Lima-Callao earthquake of $M_w \sim 8.8$ is estimated at 305 ± 40 years [1]. Currently, the confined masonry structural system is being used in low-rise buildings, particularly in regions characterized by high seismic hazard, such as in some Latin American countries [2]. An example of this is the typical configuration of Peruvian public schools, which combine confined masonry and reinforced concrete wall systems. The August 15, 2007, earthquake in Peru caused moderate to severe structural damage to 1,117 classrooms in the education sector, highlighting the vulnerability of these buildings [3].

One of the main challenges in the seismic assessment of confined masonry structures is the development of an adequate numerical model that accurately simulates the nonlinear response and predicts the failure mechanism under various seismic demands [4]. Since schools are essential buildings with a strategic role as potential shelters following an earthquake, assessing their seismic performance is crucial. Furthermore, the results obtained can be subsequently used in broader studies on seismic vulnerability and risk.

The development of nonlinear models for masonry walls has garnered significant attention from numerous researchers. For example, [5] the nonlinear behavior of masonry was represented using diagonal struts, while [6] a nonlinear model based on an equivalent frame system was employed, utilizing link-type elements. Similarly, [7] idealized the nonlinear model of the masonry wall using a concrete frame-type element, to which a shear hinge was assigned at mid-height.

This article proposes a nonlinear model for a two-story educational pavilion, featuring a reinforced concrete wall structural system in the longitudinal direction and confined masonry in the transverse direction. This model was computationally calibrated in ETABS software, using results from experimental tests.

2. BACKGROUND

Numerous researchers have dedicated significant efforts to evaluating the seismic performance of essential buildings. In this context, Cárdenas et al. [5], analyzed a '780-Pre' type school building constructed in Peru during the 1990s, characterized by a structural system that does not incorporate modern seismic-resistant design practices. The authors used SAP2000 software to perform the nonlinear static and dynamic

(time-history) analyses to study its seismic behavior. The results indicated that, in the longitudinal direction, the structure fails due to shear forces in the columns arising from the interaction with the infill masonry, while in the transverse direction transversal, the failure occurs due to compression in the masonry walls. It was concluded that the analyzed building does not ensure an adequate performance level under a severe earthquake, underscoring the need for structural retrofitting.

Gonzales et al. [7], in their study of a 60-year-old hospital built with artisanal masonry, they highlight the need to evaluate essential buildings lacking seismic-resistant design. Using a nonlinear model calibrated with laboratory tests, they performed nonlinear response-history analyses to obtain IDA curves. The results indicate that the building maintains adequate performance for accelerations below $0.35g$ (NS) and $0.40g$ (EW) but exceeds the code drift limits for accelerations above $0.40g$.

The studies by Hysenlliu & Bilgin [8] and Estêvão & Esteves [9], address the seismic performance assessment of school buildings, a critical issue in earthquake-prone regions. Hysenlliu & Bilgin evaluated the seismic performance of an unconfined masonry school building in Albania using a nonlinear static (pushover) analysis, which allowed them to obtain the capacity curve, demonstrating that the building did not meet the required performance levels and required urgent intervention to prevent collapse in the event of a severe earthquake. For its part, Estêvão & Esteves developed a computational approach to evaluate the seismic vulnerability of the "P3" school typology in southern Portugal. Using tools such as SAP2000 and SeismoStruct, they conducted a nonlinear static analysis, revealing that many of the evaluated buildings did not meet seismic regulations due to the low shear strength of the reinforced concrete columns. Both studies emphasize the importance of using nonlinear static analyses to classify the seismic safety level of school buildings, especially in vulnerable areas, and underline the need for interventions to enhance their seismic resistance.

3. METHODOLOGY

3.1. DEFINITION OF STRUCTURAL PERFORMANCE LEVELS

The performance-based method requires the designer to evaluate how a building is likely to behave during an earthquake, and its proper application helps identify unsafe designs. In addition, this approach removes arbitrary constraints and opens up

the possibility of developing safer and more cost-effective structural solutions [10].

Structural Performance (SP) establishes levels based on potential structural damage, occupant safety risks, and the building's functional capacity after a seismic event [11].

The SP levels represent specific segments of a structure's capacity curve, obtained through a nonlinear static (pushover) analysis.

To segment the capacity curve, the effective yield displacement (Δ_y) must be determined. This corresponds to the point at which up to 50% of the inelastic excursions forming the failure mechanism have been reached, without the deformation in any section exceeding 150% of the yield deformation [11]. Furthermore, the inelastic displacement (Δ_p) corresponds to the structure's lateral displacement from the effective yield point to collapse. The inelastic portion of the capacity curve is subdivided into four segments defined by fractions of (Δ_p), as shown in Fig. 1, corresponding to the following levels: Fully Operational (SP1), Operational (SP2), Life Safety (SP3), Near Collapse (SP4), and Collapse (SP5).

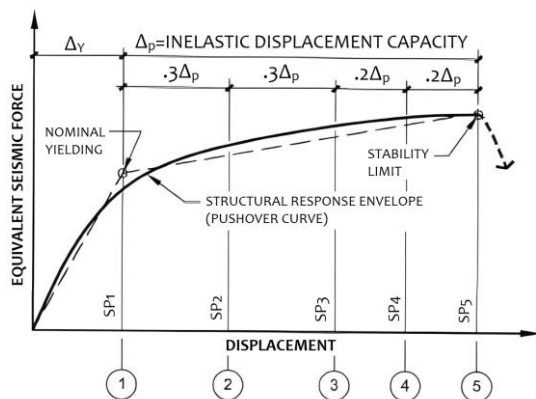


Fig. 1. Segmentation of the capacity curve [11]

3.2. MATERIAL STRESS-STRAIN CURVES

In nonlinear material modeling, it is crucial to accurately define the stress-strain curves, as they determine the structural response under extreme loads. In this study, specific models for steel and concrete were employed, optimizing the representation of the inelastic behavior of materials.

For steel, the model proposed by Park was used, as shown in Fig. 2, which considers a bilinear representation with strain hardening. This model is suitable for nonlinear analyses as it captures stiffness and strength degradation under cyclic loading [12].

For concrete, the Mander model was adopted, as shown in Fig. 3, which accounts for the effect of confinement provided by transverse reinforcement. This model is widely used to represent the enhanced

capacity of confined concrete in structural elements [12].

According to [12], indicates that by selecting the "Parametric" option, ETABS, the program used for nonlinear analysis, automatically calculates stress-strain curves based on the material properties entered, aligning with structural standards and reducing the need for manual definitions.

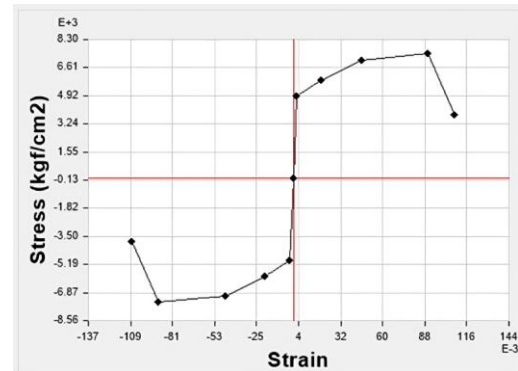


Fig. 2. Steel stress-strain curve

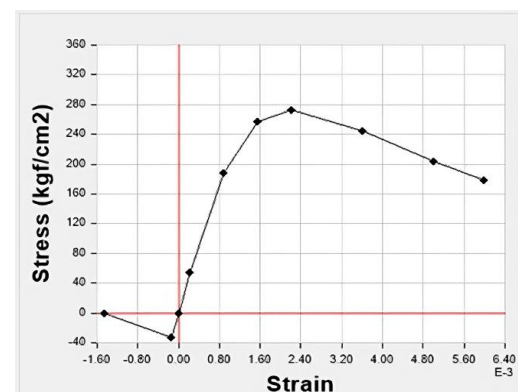


Fig. 3. Concrete stress-strain curve

3.3. NONLINEAR STATIC ANALYSIS

One of the tools for assessing the performance of low-rise educational buildings is nonlinear static analysis using the pushover method, through which lateral loads are monotonically increased on the structure until a target displacement is reached [13].

To calculate the target displacement, the capacity spectrum method can be used, which relies on equivalent linearization concepts to define an effective vibration period and equivalent viscous damping from the capacity curve. The intersection between the capacity curve and the capacity spectrum defines the target displacement [14].

In practice, the use of the capacity spectrum method for masonry structures has been utilized in various research efforts and international standards. For instance, the N2 method, a simplified variant of

the capacity spectrum approach proposed by [15], has been adopted in Eurocode 8 Part 3 for the seismic assessment of existing structures, including masonry buildings. This reflects a technical consensus that pushover procedures are useful for estimating the seismic performance of masonry buildings, provided that material-specific parameters are properly accounted for [16].

Furthermore, a study conducted by [17], implemented a performance-based design approach for a multi-story confined masonry building using the capacity spectrum method to determine the performance point. In that study, performance objectives were defined, the capacity curve was derived through a pushover analysis, and then compared against demand spectra developed from representative Peruvian earthquake records. The results allowed for verification of compliance with predefined damage limit states, demonstrating that the capacity spectrum method is applicable to confined masonry structures, as long as their actual stiffness, strength, and energy dissipation properties are accurately represented.

3.3.1. LIMITATIONS

The capacity spectrum method presents some limitations when applied to confined masonry. First, its idealization using bilinear curves fails to capture stiffness and progressive strength degradation due to cyclic damage, as well as the characteristic hysteretic pinching behavior arising from the interaction between the wall and its confinement [18], which can underestimate the real demand and lead to non-conservative results [19]. The method is suitable only for regular, geometrically simple confined masonry buildings; its application to complex or irregular structures can produce significant errors owing to torsional responses, higher-mode participation, and non-uniform distributions of mass and stiffness, thereby compromising the reliability of nonlinear static analysis results [20]. Finally, the scarcity of experimental research specifically aimed at capturing the variability in confined masonry behavior under different construction conditions limits the reliable validation of the method across a broad range of applications [21].

3.4. IDEALIZED MODEL OF CONFINED MASONRY

The Equivalent Truss Model (ETM) represents a Confined Masonry Wall (CMW) system through a framework of straight bars connected at nodes. In this manner, the masonry panels are idealized as diagonal compression struts, whose equivalent properties are derived from the transformed cross-

sectional area of the CMW. Furthermore, Reinforced Concrete (RC) confinement elements are simulated as struts or ties with fixed ends. In Fig. 4, this concept of the ETM under lateral load is illustrated. Initially, the CMW is subjected only to gravitational loads, generating axial precompression in the masonry panels and RC columns due to their role as a load-bearing wall system. As a result, an internal precompression force " P_g " develops in the diagonal members, see Fig. 4(a). When the lateral force " V " is applied, a compressive force " P_v " acts on the loaded diagonal member, and a tensile force " $-P_v$ " acts on the other diagonal member, as shown in Fig. 4(b). The compression in the loaded diagonal member will continue to increase as the lateral load " V " increases. Simultaneously, the force in the opposing diagonal member changes from compression to tension, reaching a point at which it becomes ineffective, as the masonry is unable to resist tension, see Fig. 4(c) [4].

A CMW with length " L " and height " h " can be represented by an ETM using a single diagonal strut in compression, as shown in Fig. 5(b). In this case, it is assumed that cracking in a CMW occurs along the compression diagonal when the lateral load is insufficient to induce an internal tension that compensates for the precompression effect caused by the gravitational load [4].

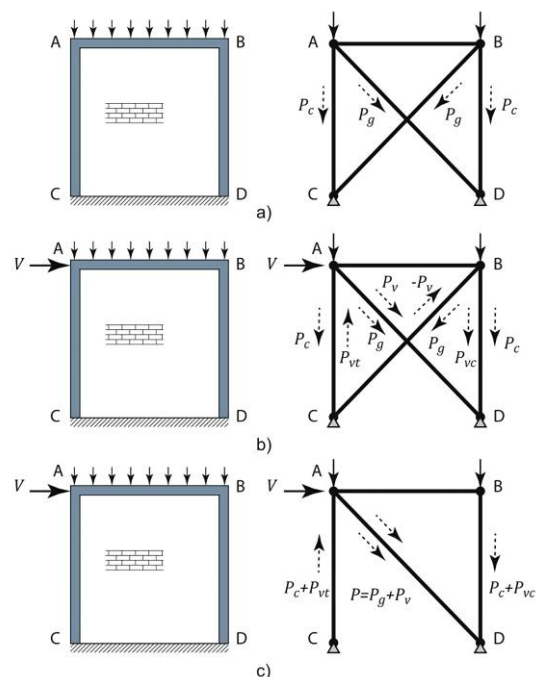


Fig. 4. Equivalent Truss Model: (a) A confined masonry wall (CMW) subjected to uniform gravity loading causing only axial compression forces P_g in the truss. (b) A CMW subjected to gravity loading and low lateral force V , hence $P_g > P_v$. (c) A CMW subjected to uniform gravity loading and sufficiently high lateral force V , such that $P_g \leq P_v$ [4].

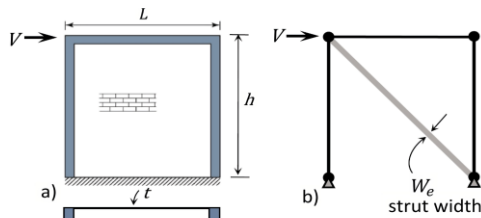


Fig. 5. Equivalent truss model (ETM) for a CM wall: a) actual CM wall. b) single-strut model [4]

According to Rankawat et al. [4], the diagonal struts must be capable of simulating the shear and flexural stiffness properties of the masonry panels. Therefore, the initial lateral stiffness “ K_L ” of the masonry wall can be calculated using the following formula:

$$K_L = \frac{1}{\frac{h_w^3}{\beta E_m I_w} + \frac{h_w}{A_v G_m}} \quad (1)$$

Where “ h_w ” is the wall height, “ E_m ” and “ G_m ” represent the masonry modulus of elasticity and shear modulus, respectively. Likewise, “ I_w ” is the moment of inertia of the wall using the transformed section, “ β ” is a coefficient that depends on the boundary condition, and “ A_v ” is the wall’s shear area. The effective width of the diagonal strut “ W_e ”, which simulates the behavior of a masonry wall with lateral stiffness “ K_L ”, can be determined using the following formula:

$$W_e = \frac{I_s^3 K_L}{t L^2 E_m} \quad (2)$$

Where “ L ” and “ t ” represent the wall’s length and thickness, respectively, and “ I_s ” is the diagonal strut length.

3.5. NONLINEAR MODEL FOR MASONRY

3.5.1. LABORATORY TESTS

In the research of Coral [22], tests were carried out on three full-scale confined masonry walls, constructed with industrial King Kong type bricks. These walls, whose dimensions are presented in Fig. 6, were subjected to cyclic lateral loads up to the point of failure. The test results are shown in Fig. 7.

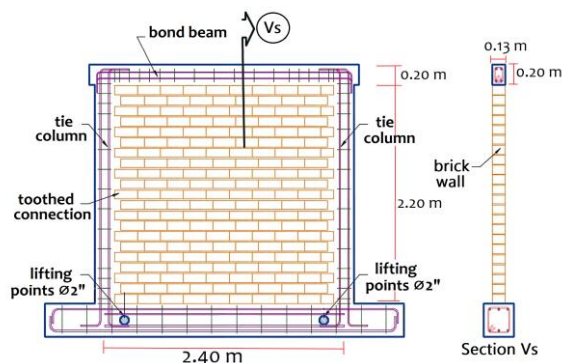


Fig. 6. Elevation and profile view of the tested wall [22]

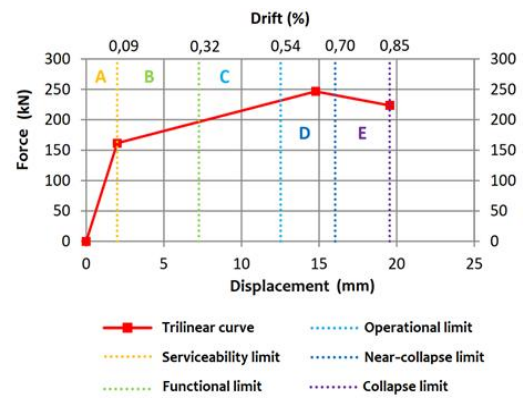


Fig. 7. Trilinear curve divided according to the damage state limits from the experimental test [22]

3.5.2. DISTORTION LIMIT VALUES

To determine the limit drift values, the relevant code principles were reviewed [23]. According to this, the linear response limit is set at 1/800, while the maximum drift allowing for masonry repairs is 1/200. If this value is exceeded, the structure is considered not repairable. Given that the Standard [23], It only provides information on the drift up to which the masonry can be repaired. Tests were consulted to identify the ultimate drift that confined masonry can reach, finding a value of 1/115, as noted by [24].

3.5.3. FORMULATION FOR ESTIMATING LIMIT STATES

According to the study conducted by [2], the lateral strength of confined masonry walls depends on various parameters related to material properties, geometric characteristics, and loading conditions. In his research, the author proposed a relationship to estimate the trilinear lateral load–deformation curve for this type of wall, as shown in Fig. 8. In the present study, the trilinear curve proposed by [2] is adopted as a reference model; however, adjustments are made to the lateral load parameters in order to calibrate the numerical results with respect to the experimental test conducted by Coral [22]. To achieve this calibration, the equivalent diagonal strut model with a trilinear force–deformation constitutive law was employed. The calibration process involved manual and iterative adjustment of the parameters defining the trilinear curve until the numerical response closely matched the experimental results reported by Coral [22]. This procedure enabled an adequate representation of the nonlinear behavior of the masonry wall, including the initial stiffness (represented by the slope from the origin to point A), the maximum lateral strength reached at point B, and the progressive strength degradation in the post-peak branch between points B and C, as shown in Fig. 9. The calibration also considered the type of masonry unit, the mechanical properties, and the

geometric dimensions of the tested specimen, resulting in a consistent match between the numerical model and the available experimental data.

The shear strength value of the masonry wall “ V_m ” is obtained from [23].

$$V_m = 0.5 v'_m \alpha t L + 0.23 P_g \dots \dots \dots (3)$$

where: “ v'_m ” is the characteristic shear strength of the masonry, “ α ” is the shear strength reduction factor due to slenderness effects, “ t ” is the effective wall thickness, “ L ” is the total length of the wall, and “ P_g ” is the service gravitational load.

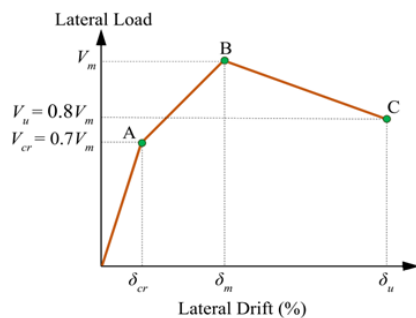


Fig. 8. Recommended idealized tri-linear lateral load – deformation curve for confined masonry walls [2]

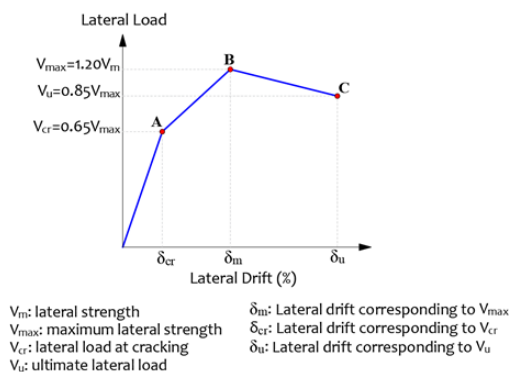


Fig. 9. Calibrated trilinear lateral load–deformation curve for confined masonry walls

3.5.4. AXIAL FORCE – DEFORMATION RELATIONSHIP

Equilibrium is used to relate the lateral force to the axial force (see Fig. 10), with the aim of transforming a force–displacement model, as shown by the test results of [22] into an axial force–deformation model. For this purpose, the following equation is employed:

$$P = \frac{V}{\cos \theta} \dots \dots \dots (4)$$

where: “ P ” denotes the axial force, “ V ” the lateral force, and “ θ ” the inclination angle of the diagonal strut.

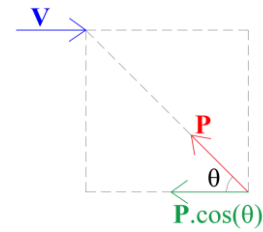


Fig. 10. Relationship between lateral force “ V ” and axial force “ P ”

3.5.5. CALIBRATION OF THE NONLINEAR MODEL

The idealization of the nonlinear mathematical model of the masonry wall was carried out using a rectangular concrete frame element, whose dimensions and linear properties were obtained from [22]. An axial hinge “ P ” was assigned to this element at its mid-length, where the force and displacement parameters obtained by transforming the shear–displacement model into an axial–deformation model were defined. Furthermore, a rigid zone factor of one was included in the upper beam. The Fig. 11(a) and 11(b) illustrates both the schematic of the tested masonry wall and the equivalent truss model proposed in this study. Finally, Fig. 12 presents a comparison between the trilinear capacity curve obtained from the laboratory test and that of the equivalent model, demonstrating an appropriate similarity.

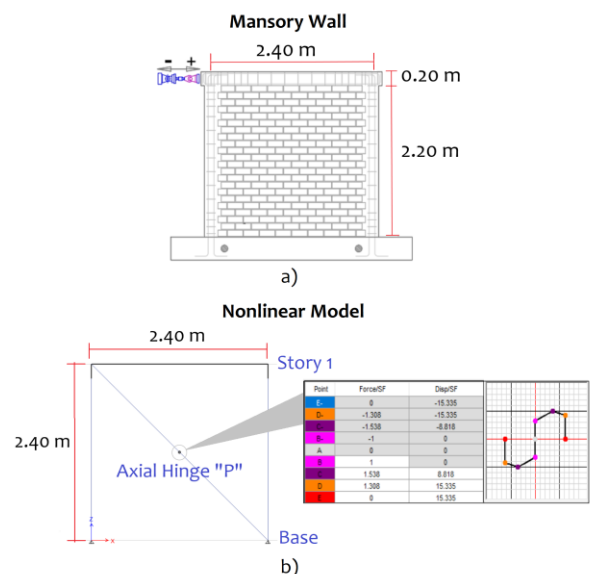


Fig. 11. Modeling of the confined masonry wall and its equivalent nonlinear truss model: (a) Schematic of the tested confined masonry wall with its geometric dimensions [22]. (b) Equivalent nonlinear truss model used in the analysis, including an axial hinge “ P ”.

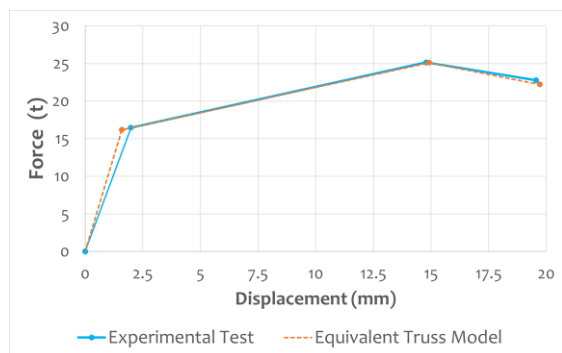


Fig. 12. Calibration of the equivalent truss model

3.6. DYNAMIC NONLINEAR ANALYSIS

Nonlinear dynamic analysis allows for a more accurate calculation of the structural response to earthquakes, by including the inelastic behavior of the elements under cyclic ground motions. Unlike nonlinear static analysis, dynamic analysis explicitly represents hysteretic energy dissipation in the inelastic range, thereby reducing the number of required assumptions. However, the accuracy depends on the quality of the model and its ability to capture the significant effects of the structural behavior [14].

For time-history dynamic analysis, at least three acceleration records must be used, each containing the ground acceleration history in two perpendicular directions. Besides, the average square root of the sum of the squares (SRSS) of all records must be equal to or greater than the code's elastic spectrum ($R=1$) in the range of 0.2 to 1.5 times the building's fundamental period. In the case of using three to six records, the structural demand is taken as the maximum recorded value of the peak responses, whereas for seven or more records, the average of these responses can be utilized [25].

Following the recommendations of [25], three pairs of seismic records were selected, prioritizing recording stations located on soils like type S3, since the educational institution is situated on this type of soil. Table I presents the selected seismic records, their corresponding stations, and the peak acceleration values for each component. These records were subsequently spectrally adjusted to ensure compatibility with the site's elastic spectrum.

Hysteresis is the process of energy dissipation through inelastic deformation. To describe this behavior in different materials, various hysteresis models are employed. In the present study, the Takeda model, widely accepted for representing the cyclic behavior of reinforced concrete elements [26].

Although originally developed based on tests of reinforced concrete elements, the Takeda model has been used for modeling confined masonry walls due to certain similarities in their behavior. Both systems exhibit cracking that leads to a progressive reduction in stiffness, and can develop a certain degree of

ductility before strength degradation occurs. Some studies have adopted this model to simulate the behavior of confined masonry walls in nonlinear dynamic analyses. For instance, in the study by [27], the author employs a Takeda-type hysteresis curve to reproduce stiffness and strength degradation under cyclic loading. This strategy can capture the progressive stiffness degradation in each cycle as the wall cracks, as well as the reduction in strength in subsequent cycles, through the calibration of the monotonic envelope curve based on experimental tests [28].

Practical justification for this approach lies in the absence of specific hysteretic models for confined masonry in commercial structural analysis platforms. As a result, the Takeda model is adopted as an operational alternative due to certain qualitative similarities in cyclic behavior [28]. However, this extrapolation involves important limitations. The model was originally developed for reinforced concrete elements, and its application to confined masonry walls lacks direct and specific experimental validation. To date, there is no sufficiently broad and systematized experimental database confirming that this model accurately captures the mechanisms of stiffness and strength degradation typical of confined masonry under cyclic loading. Although some studies have employed the Takeda model for this purpose, its use is primarily based on convenience or calibration criteria, rather than on rigorous empirical validation. In the present study, it was not possible to access detailed and representative experimental data that would allow for a more robust calibration. Therefore, the use of this model should be understood as a preliminary approximation, subject to inherent uncertainties, and whose accuracy could be improved with future experimental evidence.

3.6.1. LIMITATIONS

The use of the Takeda hysteresis model without proper calibration can lead to significant inaccuracies in estimating the seismic response of confined masonry structures. First, ductility may be overestimated, as masonry exhibits lower deformation capacity and more pronounced strength degradation compared to reinforced concrete [29]. Similarly, the effective stiffness may be inaccurately predicted, since masonry experiences a faster reduction in stiffness during the initial loading cycles [28]. In addition, the model may underestimate cumulative damage by failing to adequately represent the cyclic degradation characteristic of this material [30]. Therefore, careful model calibration and the inclusion of experimental validations are recommended to ensure more realistic results [28]. Finally, Table II presents the mechanical properties of the materials employed in the equivalent model.

TABLE I
Selected stations

Seismic Record	Name of Station	Station Location	PGA E-W (cm/s ²)	PGA N-S [cm/s ²]
Pisco 15/08/2007	UNICA	San Luis Gonzaga National University, Ica	-272.82	333.66
Atico 17/07/2017	SCARQ	SENCICO, Arequipa	-41.59	-43.86
Atacama 18/07/2024	SCTAC	SENCICO, Tacna	5.80	6.82

TABLE II
Mechanical properties

Material	Expected compressive strength (kg/cm ²)	Modulus of Elasticity (kg/cm ²)	Hysteretic Model
Concrete Column	$f'_c=273$	2.478×10^5	Takeda
Concrete Beam	$f'_c=273$	2.478×10^5	Takeda
Masonry	$f'_m=65$	3.25×10^4	Takeda
Reinforcing Steel	-	2.039×10^6	Kinematic

4. CASE STUDY DESCRIPTION

This study evaluated Pavilion 02-R of Educational Institution No. 22459, Julio C. Tello. This two-story building has a floor area of 31.20 m × 9.75 m and consists of four classrooms on each level, as shown in Fig. 13. The structure consists of a system of reinforced concrete walls in the longitudinal direction and a confined masonry system in the transverse direction, constructed using industrial King Kong-type bricks. The institution is located in the district of Pisco, in the department of Ica, a high-seismicity area according to [25]. It should be noted that the pavilion was constructed in 2010, following the 2007 earthquake, whose epicenter was located 40 km west of the city of Pisco in Peru. The dimensions and detailing of the steel for the different structural elements are presented in Fig. 14.

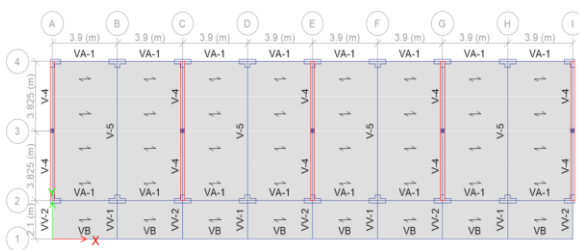


Fig. 13. Plan view of the structure model in ETABS

COLUMN DETAIL			
TYPE	C-1	C-2	C-3
SECTION			
STEEL	4Ø3/4" + 2Ø5/8"	4Ø3/4" + 2Ø5/8"	4Ø3/4" + 2Ø5/8"
STIRRUP	2Ø3/8": 1@0.05, 7@0.10, Rem.@0.20 m	3Ø3/8": 1@0.05, 10@0.10, Rem.@0.20 m	

BEAM DETAIL			
TYPE	VA-1	V-4	V-5
SECTION			
STEEL	3Ø5/8"	3Ø5/8"	5Ø5/8"
STIRRUP	Ø3/8": 1@0.05, 10@0.10, Rem.@0.25 m		2Ø3/8": 1@0.05, 14@0.10, Rem.@0.20 m

Fig. 14. Detailing of structural elements

4.1. CALIBRATION OF THE LINEAR MODEL

Based on the equations described in Section 3.4, the effective width of the diagonal strut was determined to be $W_e = 3.43$ m. To validate the equivalent truss linear model, it is necessary to perform a calibration by comparing it with a model that represents the masonry using shell thin elements, see Fig. 15(a) and 15(b). The comparison considers the periods, mass, and lateral displacements under an applied lateral load, with the purpose of adequately capturing the axial stiffness of the walls (see Table III). In traditional designs, confined masonry walls are modeled using shell thin-type elements, and the incorporation of diagonal struts through frame-type elements in the equivalent truss model aims to preserve this axial stiffness. Therefore, variations were introduced in the stiffness modification factors of the frame-type elements, increasing on average the axial stiffness by 35% and reducing weight and mass by 25%.

TABLE III
Calibration of linear model of masonry walls

Comparison parameters		Modeling Shell-Thin	Modeling Frame	Sim. (%)
Period	Mode 1	0.172 s	0.172 s	100 %
	Mode 2	0.083 s	0.083 s	100 %
Story weight	Story 2	185.35 t	185.15 t	99,9 %
	Story 1	335.45 t	335.25 t	99,9 %
Lateral disp.	Story 2	0.747 mm	0.748 mm	99,9 %
	Story 1	0.408 mm	0.408 mm	100 %

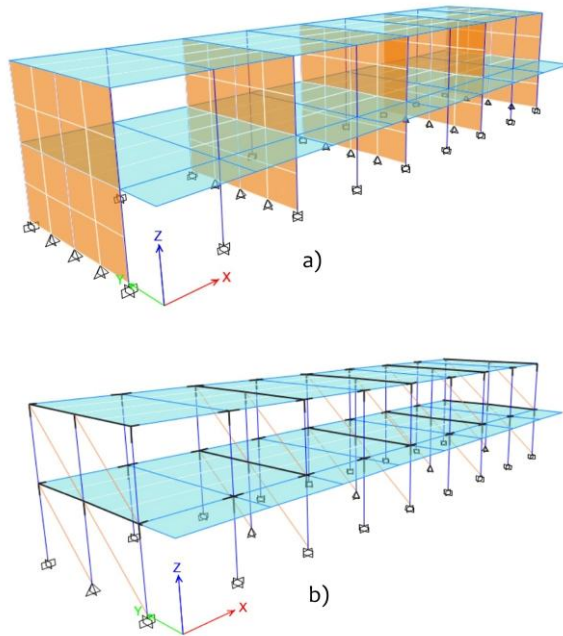


Fig. 15. Modeling of confined masonry walls: (a) Using shell thin-type elements. (b) Using frame-type elements.

4.2. PLASTICITY MODELS

The plasticity model employed for confined masonry corresponds to a concentrated axial hinge "P". The force and displacement values associated with this model were calculated following the guidelines outlined in Sections 3.4 and 3.5. The hinge is located at the mid-length of the diagonal struts, and its values vary according to the axial load " P_g " acting on each confined masonry wall. On the other hand, the plasticity model adopted for the columns corresponds to a distributed fiber section type, which distributes plasticity through numerical integrations performed across the cross sections and along the length of the member [14]. Fig. 16 shows the fibers for hinge of the "C-2" column.

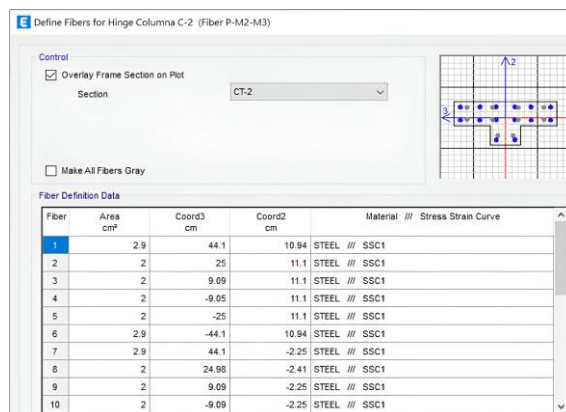


Fig. 16. Fibers for hinge of the "C-2" column

The selected plasticity model for the beams is the concentrated hinge type, where plasticity is concentrated in zero-length hinges using parameters based on moment-rotation models. These elements feature relatively compact and numerically efficient formulations [14]. Fig. 17 shows the plastic hinge properties of the "V-5" beam.

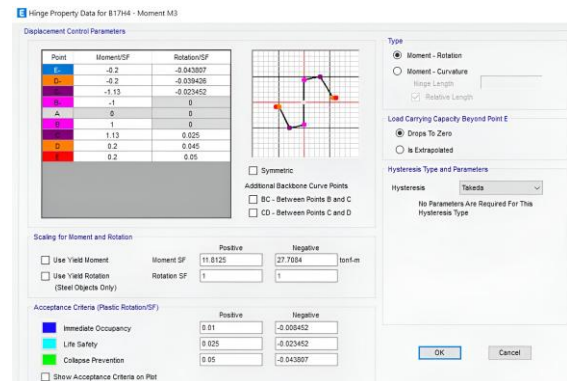


Fig. 17. Hinge properties of the "V-5" beam

4.3. PROPERTIES OF PLASTIC HINGES IN DIAGONAL STRUTS

In the diagonal struts, a plastic hinge is assigned at the midpoint of their length. The properties of this hinge are determined based on the axial load obtained from the linear analysis, which varies depending on the level at which the wall is located.

The following describes the calculation of the properties of a plastic hinge corresponding to a diagonal strut representing a confined masonry wall located on the exterior of the structure:

4.3.1. GENERAL DATA

The dimensions and mechanical properties of the materials shown in Table IV were taken from the project of Educational Institution No.22459, which comply with the guidelines specified in [23].

TABLE IV
Confined masonry wall parameters

Parameters	Description	Values
Mechanical properties	Shear strength ($v'm$)	8.1 kg/cm²
	Compressive strength ($f'm$)	65 kg/cm²
	Modulus of elasticity (E_m)	32500 kg/cm²
	Shear Modulus (G_m)	13000 kg/cm²
Wall dimensions	Wall length (L)	7.65 m
	Wall height (h)	3.35 m
	Wall thickness (e)	0.23 m
	Angle of inclination (θ)	41.21°
Other parameters	Axial load (P_g)	24.70 t
	Slenderness factor (α)	1

4.3.2. SHEAR STRENGTH OF THE WALL

The shear strength of the wall (V_m) is calculated using the equation (3) established in Section 3.5.3.

$$V_m = 76.94 t \dots\dots\dots(5)$$

4.3.3. LIMIT STATES OF LATERAL FORCE

Due to the inherent variations in masonry across different countries, determined by material properties, joint element details, and construction practices, it is necessary to adjust the relationship of the trilinear lateral load–deformation curve. Section 3.5.3. presented a proposal supported by tests conducted in Peru was presented, modifying the original curve introduced in the study by [2].

$$V_{max} = 1.20V_m = 92.32 t \dots\dots\dots(6)$$

$$V_u = 0.85V_{max} = 78.48 t \dots\dots\dots(7)$$

$$V_{cr} = 0.65V_{max} = 60.01 t \dots\dots\dots(8)$$

4.3.4. RELATIONSHIP BETWEEN SHEAR FORCE “V” AXIAL LOAD “P”

Applying the relationship presented in Section 3.5.4. and considering that the axial load is distributed between two diagonal struts, it is divided by two. Based on this, the following values are obtained:

$$P_{cr} = \frac{V_{cr}}{2 \cos \theta} = 39.88 t \dots\dots\dots(9)$$

$$P_{max} = \frac{V_{max}}{2 \cos \theta} = 61.37 t \dots\dots\dots(10)$$

$$P_u = \frac{V_u}{2 \cos \theta} = 52.16 t \dots\dots\dots(11)$$

The results are expressed in terms of the cracking force, P_{cr} , yielding the following values:

$$\frac{P_{max}}{P_{cr}} = 1.538 \dots\dots\dots(12)$$

$$\frac{P_u}{P_{cr}} = 1.308 \dots\dots\dots(13)$$

4.3.5. RELATIONSHIP BETWEEN DRIFTS “ δ ” AND DEFORMATIONS “D”

The drifts defined in Section 3.5.2. will serve as the basis for estimating the deformations associated with each damage state.

$$\delta_{cr} = \frac{1}{800} \dots\dots\dots(14)$$

$$\delta_{max} = \frac{1}{200} \dots\dots\dots(15)$$

$$\delta_u = \frac{1}{115} \dots\dots\dots(16)$$

$$D_{cr} = \delta_{cr} h \cos \theta = 3.15 mm \dots\dots\dots(17)$$

$$D_{max} = \delta_{max} h \cos \theta = 12.601 mm \dots\dots\dots(18)$$

$$D_u = \delta_u h \cos \theta = 21.914 mm \dots\dots\dots(19)$$

4.3.6. ACCEPTANCE CRITERIA

Fig. 7 presents the experimental results of [22], where acceptance criteria are established based on a percentage of the drift. This relationship is then applied to determine the performance levels as a function of displacement.

$$SP1 = \frac{0.09}{100} \cos \theta h = 2.268 mm \dots\dots\dots(20)$$

$$SP3 = \frac{0.54}{100} \cos \theta h = 13.609 mm \dots\dots\dots(21)$$

$$SP4 = \frac{0.70}{100} \cos \theta h = 17.641 mm \dots\dots\dots(22)$$

4.3.7. PROPERTIES OF THE PLASTIC HINGE IN ETABS SOFTWARE

The properties calculated in Sections 4.3.1 to 4.3.6 are incorporated into the ETABS software, as illustrated in Fig. 18. This procedure allows the nonlinear behavior to be represented through concentrated hinges located at the mid-length of the diagonal struts. Finally, Fig. 19 shows plastic hinge placement in the global structure.

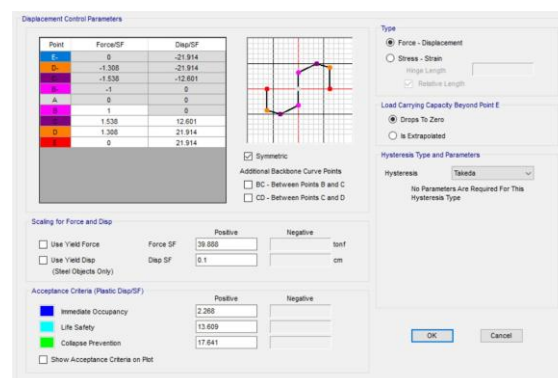


Fig. 18. Plastic hinge properties: exterior masonry wall

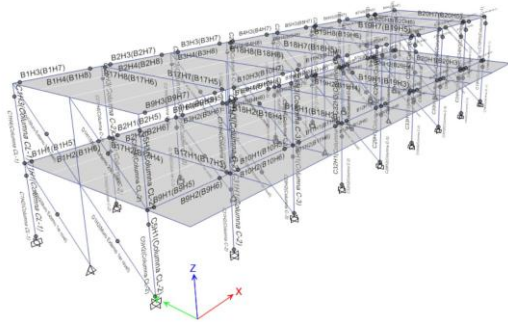


Fig. 19. Placement of plastic hinges in structural elements

5. RESULTS

5.1. SEGMENTED CAPACITY CURVE

Before an earthquake, structures are subjected only to gravitational loads, followed by seismic actions. Therefore, a “Gravity Load” case must be defined in ETABS, including 100% dead load, 50% live load on typical floors, and 25% live load on the roof, as specified in [31]. A control point should also be selected near the center of mass at the roof level; in this case, point No. 4 was chosen, located at the intersection of gridlines 3 and E.

To determine the bilinear curve used to segment the capacity curve into different seismic performance levels, the coefficient method was employed, as shown in Fig. 20 and 21. This method is based on the energy equivalence principle, which states that the area under the idealized bilinear curve must be equivalent to the area under the actual curve obtained from nonlinear static analysis. In this way, the simplified curve preserves the energy dissipation capacity of the structural system, accurately representing its inelastic behavior without the need for excessively detailed or complex modeling. This approach is particularly useful in performance-based evaluations, where balancing analytical accuracy and computational efficiency is essential [32]. The capacity curve was segmented based on the model proposed by SEAOC, using the inelastic displacement of the structure (Δ_p) as the defining parameter, as shown in Fig. 24 and 25.

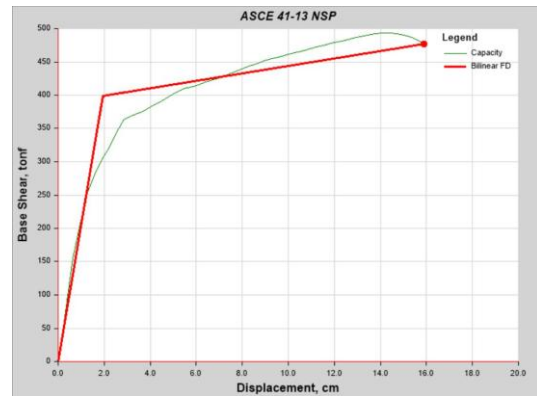


Fig. 20. Bilinear curve in the X direction

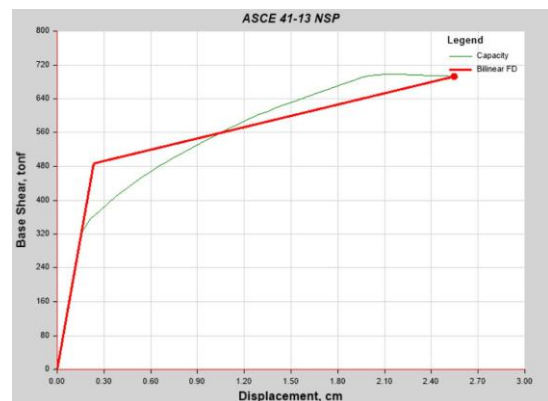


Fig. 21. Bilinear curve in the Y direction

5.2. PERFORMANCE POINT

The performance point was determined using the Capacity Spectrum Method, as shown in Fig. 22 and 23. In the X direction, the parameters used were: spectral acceleration (S_a) of 1.059 g, spectral displacement (S_d) of 7.09 cm, and effective damping (β_{eff}) of 0.2049. In the Y direction, S_a and S_d values of 1.06 g and 1.09 cm, respectively, were employed, with a β_{eff} of 0.2047. Regarding the damping ratio adopted for the construction of the response spectrum, a value of 5% was considered, in accordance with the Peruvian technical standard E.030. However, this standard is general in nature and does not specify the type of material to which this value applies [25].

The results of the performance point by the capacity spectrum method which produced displacements of 9.02 cm in the X direction and 1.17 cm in the Y direction, with base shears of 451.97 t and 540.24 t, respectively. These results, representing the structural response to a Maximum Considered Earthquake (MCE) associated with a return period of 2,475 years, correspond to the most severe seismic hazard scenario according to reference [31].

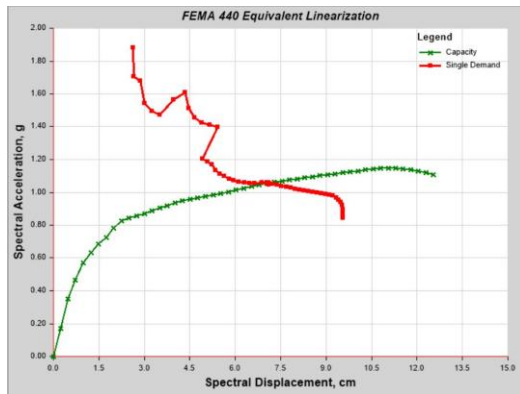


Fig. 22. Capacity spectrum method in X direction

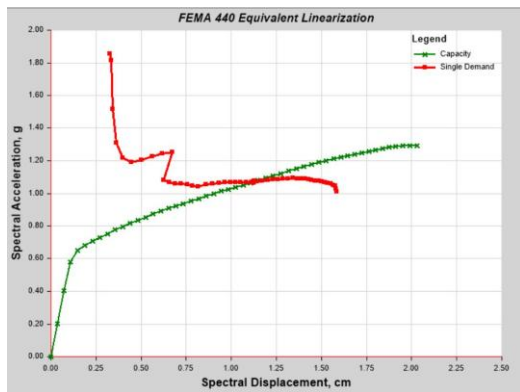


Fig. 23. Capacity spectrum method in Y direction

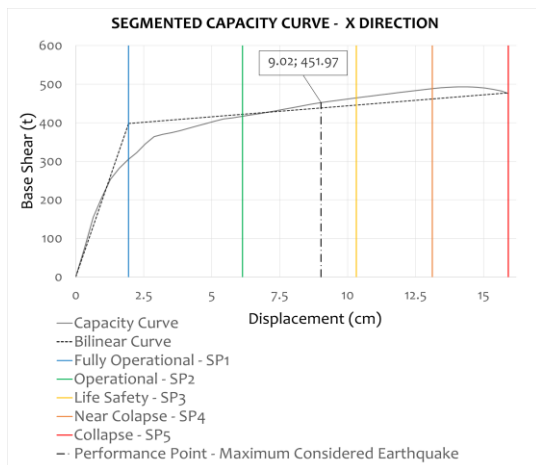


Fig. 24. Segmented capacity curve in X direction

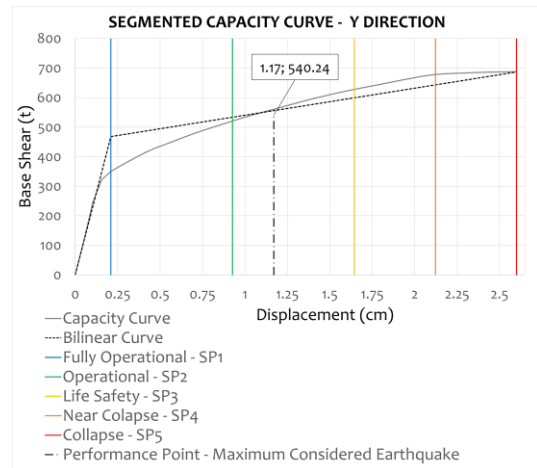


Fig. 25. Segmented capacity curve in Y direction

5.3. ANALYSIS TIME HISTORY

Tables V and VI present the results of the nonlinear time-history analysis conducted using the seismic records selected for the study. The maximum displacement observed is 8.14 cm in the X direction and 1.41 cm in the Y direction. Similarly, the maximum base shear force shows values of 406.78 t in the X direction and 501.21 t in the Y direction.

The comparison of lateral displacements obtained from the nonlinear static and dynamic analyses showed good agreement: 90.2% in the X direction and 82.9% in the Y direction. Similarly, the base shear forces showed a similarity of 90.0% in the X direction and 92.7% in the Y direction, confirming the consistency of both approaches.

TABLE V
Analysis time-history in X direction



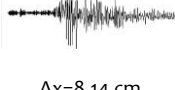









Seismic Record	Displacement Max.	Base Shear Max.
Pisco 15/08/2007	 $\Delta x = 6.49$ cm	 $V_x = 356.64$ t
Atico 17/07/2017	 $\Delta x = 8.14$ cm	 $V_x = 406.78$ t
Atacama 18/07/2024	 $\Delta x = 7.62$ cm	 $V_x = 384.29$ t

TABLE VI
Analysis time-history in Y direction

Seismic Record	Displacement Max.	Base Shear Max.
Pisco 15/08/2007	 $\Delta y=1,10$ cm	 $V_y=449.72$ t
Atico 17/07/2017	 $\Delta y=1,41$ cm	 $V_y=501.21$ t
Atacama 18/07/2024	 $\Delta y=1,19$ cm	 $V_y=455.47$ t

CONCLUSIONS

- In this research work, nonlinear static and time-history dynamic analyses were performed to determine the seismic performance of a two-story public educational institution. A computational model was proposed in ETABS software to simulate the nonlinear behavior of the masonry wall, using a diagonal frame-type element that incorporates an axial hinge at mid-length in the lateral deformation direction. This model was calibrated based on experimental tests conducted in the laboratory, which allowed for the validation of its viability as an alternative to represent the nonlinear behavior of masonry walls.
- The seismic performance assessment of Public Educational Institution No.22459 through nonlinear static and dynamic analyses, presented significant findings that contribute to a global understanding of the behavior of buildings made up of confined masonry and reinforced concrete wall structural systems. In both directions, the most unfavorable scenario was evaluated, achieving the performance level corresponding to life safety for a maximum considered earthquake with a return period of 2475 years.
- The particularities of masonry in each country, stemming from material properties, construction details, and employed techniques, make it essential to adapt the trilinear curve relationship describing lateral load-deformation. Furthermore, it is essential to calibrate the equivalent truss model in the linear analysis by adjusting the modification factors that allow varying the

axial stiffness, weight and mass of the diagonal struts representing the masonry walls. These adaptations are essential to ensure a more accurate analysis according to local conditions.

- The use of the Takeda hysteresis model and seismic assessment methods originally developed for reinforced concrete in structural masonry buildings is viable, but it requires experimental justification and proper calibration. Otherwise, inaccurate results may be obtained, particularly in terms of ductility, stiffness, and cumulative damage. It is recommended to perform experimental validations or apply empirical adjustments to improve the accuracy of the structural assessment. Furthermore, it is essential to understand the limitations and implications of these adaptations to ensure a safe and efficient design.

REFERENCES

- [1] J. C. Villegas-Lanza et al., "Active tectonics of Peru: Heterogeneous interseismic coupling along the Nazca megathrust, rigid motion of the Peruvian Sliver, and Subandean shortening accommodation," *J Geophys Res Solid Earth*, vol. 121, no. 10, pp. 7371–7394, Oct. 2016, doi: 10.1002/2016JB013080.
- [2] B. Borah, H. B. Kaushik, and V. Singhal, "Lateral load-deformation models for seismic analysis and performance-based design of confined masonry walls," *Journal of Building Engineering*, vol. 48, 2022, doi: 10.1016/j.jobe.2021.103978.
- [3] Instituto Nacional de Defensa Civil, "Impacto Socioeconómico y Ambiental del Sismo del 15 de agosto de 2007," Lima, Perú, 2011. [En línea]. Disponible: <https://biblioteca.igp.gob.pe/bib/13476>
- [4] N. Rankawat, S. Brzev, S. K. Jain, and J. J. Pérez Gavilán, "Nonlinear seismic evaluation of confined masonry structures using equivalent truss model," *Eng Struct*, vol. 248, 2021, doi: 10.1016/j.engstruct.2021.113114.
- [5] O. Cardenas, A. Farfan, G. Huaco, and A. Stavridis, "Seismic Performance Assessment of a Typical Peruvian Public-School Building," in *IOP Conference Series: Materials Science and Engineering*, 2021. doi: 10.1088/1757-899X/1048/1/012014.
- [6] L. Pasticier, C. Amadio, and M. Fragiocomo, "Non-linear seismic analysis and vulnerability evaluation of a masonry building by means of the SAP2000 V.10 code," *Earthq Eng Struct Dyn*, vol. 37, no. 3, pp. 467–485, 2008, doi: 10.1002/EQE.770.
- [7] G. Gonzales, A. Aguilar, and G. Huaco, "Incremental dynamic analysis of a 60 year old hospital with handmade brick masonry walls," *Proceedings of the LACCEI international Multi-conference for Engineering, Education and Technology*, 2020, doi: 10.18687/LACCEI2020.1.1.375.
- [8] M. Hysenliu and H. Bilgin, "Seismic performance assessment of a typified school building damaged during the 2019 Albanian earthquakes," *IOP Conf Ser Mater Sci Eng*, vol. 989, no. 1, Dec. 2020, doi: 10.1088/1757-899X/989/1/012030.
- [9] J. M. C. Estêvão and C. Esteves, "Nonlinear seismic analysis of existing RC school buildings: The 'P3' school typology," *Buildings*, vol. 10, no. 11, pp. 1–16, 2020, doi: 10.3390/buildings10110210.
- [10] M. Willford, A. Whittaker, and R. Klemencic, *Recommendations for the Seismic Design of High-Rise Buildings*. 2008, doi: 10.13140/RG.2.1.2798.8085.
- [11] Seismology Committee Structural Engineers Association of California, *Recommended Lateral Force Requirements and Commentary*, Sixth Edition. California: Structural Engineers Association of California (SEAOC), 1996. [Online]. Available: <https://archive.org/details/gov.law.seac.blue.1996>

- [12] Computers & Structures Inc., "CSI Analysis Reference Manual," Nov. 2017. [Online]. Available: <https://es.scribd.com/document/872518082/Analysis-Reference>
- [13] A. Parammal Vatteri and D. D'Ayala, "Classification and seismic fragility assessment of confined masonry school buildings," *Bulletin of Earthquake Engineering*, vol. 19, no. 5, pp. 2213–2263, 2021, doi: 10.1007/s10518-021-01061-9.
- [14] NIST GCR 10-917-5, "Nonlinear Structural Analysis For Seismic Design - A Guide for Practicing Engineers," 2010. [Online]. Available: https://www.researchgate.net/publication/304395056_Nonlinear_Structural_Analysis_for_Seismic_Design_-_A_Guide_for_Practicing_Engineers
- [15] P. Fajfar and F. MA, "N2-A Method for Nonlinear Seismic Analysis of Regular Buildings," vol. 5, Jan. 1988. [Online]. Available: https://www.researchgate.net/publication/246913483_N2-A_Method_for_Nonlinear_Seismic_Analysis_of_Regular_Buildings
- [16] G. Guerrini, S. Kallioras, S. Bracchi, F. Graziotti, and A. Penna, "Displacement Demand for Nonlinear Static Analyses of Masonry Structures: Critical Review and Improved Formulations," *Buildings* 2021, Vol. 11, Page 118, vol. 11, no. 3, p. 118, Mar. 2021, doi: 10.3390/BUILDINGS11030118.
- [17] R. D. Santana Tapia, "Diseño sísmico por desempeño de estructuras de albañilería confinada," master's thesis, Universidad Nacional de Ingeniería, Lima, Perú, 2012. [Online]. Available: <http://hdl.handle.net/20.500.14076/1156>
- [18] R. Perez-Martinez and L. and Esteva, "A New Model for Hysteretic Behavior and Damage for Confined Masonry Walls," *Journal of Earthquake Engineering*, vol. 15, no. 6, pp. 942–958, Jul. 2011, doi: 10.1080/13632469.2010.544374.
- [19] T. Spyridon, "Pushover analysis for seismic assessment and design of structures," 2008, Accessed: Jun. 28, 2025. [Online]. Available: <https://www.ros.hw.ac.uk/handle/10399/2170>
- [20] M. Sukrawa, G. Pringgana, and P. Yustinaputri, "Modelling of confined masonry structure and its application for the design of multi-story building," *MATEC Web of Conferences*, vol. 276, p. 01034, Mar. 2019, doi: 10.1051/mateconf/201927601034.
- [21] J. J. Pérez Gavilán Escalante, S. Brzev, E. F. Espinosa Cazarín, S. Ganzerli, D. Quiun, and M. T. Reiter, "Experimental Research Studies on Seismic Behaviour of Confined Masonry Structures: Current Status and Future Needs," *Buildings*, vol. 13, no. 7, 2023, doi: 10.3390/buildings13071776.
- [22] M. Coral, "Ensayos cíclicos en muros de albañilería confinada construidos con ladrillo king kong de fabricación industrial," thesis, Pontificia Universidad Católica del Perú, Lima, Perú, 2018. [Online]. Available: <http://hdl.handle.net/20.500.12404/13133>
- [23] Servicio Nacional de Capacitación para la Industria de la Construcción, "Norma E.070 - Albañilería," Lima, Perú, 2020. [Online]. Available: <https://cdn.www.gob.pe/uploads/document/file/2366661/56%20E.070%20ALBA%20%91LERIA.pdf>
- [24] Á. San Bartolomé, "Comportamiento Sísmico Experimental de la Albañilería - Tercera Etapa," Lima, Perú, 2011. Accessed: Jun. 23, 2025. [Online]. Available: <http://blog.pucp.edu.pe/blog/albanileria/>
- [25] Servicio Nacional de Capacitación para la Industria de la Construcción, "Norma E.030 - Diseño Sismorresistente," Lima, Perú, 2020. [Online]. Available: https://cdn-web.construccion.org/normas/rne2012/rne2006/files/titulo3/02_E/2018_E030_RM-355-2018-VIVIENDA_Peruano.pdf
- [26] A. Ilki and N. Kumbasar, *Hysteresis Model for Reinforced Concrete Members*. [Online]. Available: 2000.https://www.researchgate.net/publication/258837391_Hysteresis_Model_for_Reinforced_Concrete_Members
- [27] S. Sáenz, "Curvas de fragilidad de estructuras de albañilería confinada empleando la base de registros sísmicos chilenos," thesis, Universidad de Chile, Santiago de Chile, Chile, 2018. [Online]. Available: <https://repositorio.uchile.cl/handle/2250/159573>
- [28] J. Cisterna, "Metodología para a evaluación del desempeño sísmico de viviendas sociales en albañilería confinada," master's thesis, Pontificia Universidad Católica de Chile, Santiago de Chile, Chile, 2015. [Online]. Available: https://masterieg.uc.cl/wp-content/uploads/2022/04/2015-10_JOS%C3%89_ANDR%C3%89S_CISTERNA_TOLEDO.pdf
- [29] P. Lestuzzi and M. Badoux, "The gamma-model: A simple hysteretic model for reinforced concrete walls," May 2003. [Online]. Available: https://www.researchgate.net/publication/37450365_The_gamma_model_A_simple_hysteretic_model_for_reinforced_concrete_walls
- [30] G. Torrisi, "Análisis y diseño de estructuras de hormigón armado y mampostería," doctoral thesis, Universidad Nacional de Cuyo, Mendoza, Argentina, 2013. doi: 10.13140/RG.2.1.3634.0083.
- [31] ASCE, *Seismic Evaluation and Retrofit of Existing Buildings*. American Society of Civil Engineers, 2017. doi: 10.1061/9780784414859.
- [32] H. Elgohary, "A simplified trilinear concrete stress-strain curve: energy-based modeling of experimental data compliant with various codes," *Journal of Umm Al-Qura University for Engineering and Architecture*, Mar. 2025, doi: 10.1007/s43995-025-00117-0.



Los artículos publicados por la TECNIA se distribuyen bajo la licencia de uso Creative Commons (CC BY 4.0). Permisos lejos de este alcance pueden ser consultados a través del correo tecnia@uni.edu.pe